



## Feature-based attention enhances performance by increasing response gain

Katrin Herrmann<sup>a</sup>, David J. Heeger<sup>a,b</sup>, Marisa Carrasco<sup>a,b,\*</sup>

<sup>a</sup> Department of Psychology, New York University, United States

<sup>b</sup> Center for Neural Science, New York University, United States

### ARTICLE INFO

#### Article history:

Received 17 January 2012

Received in revised form 20 April 2012

Available online 2 May 2012

#### Keywords:

Feature-based attention

Contrast

Attention models

Response gain

Orientation discrimination

Contrast gain

### ABSTRACT

Covert spatial attention can increase contrast sensitivity either by changes in contrast gain or by changes in response gain, depending on the size of the attention field and the size of the stimulus (Herrmann et al., 2010), as predicted by the normalization model of attention (Reynolds & Heeger, 2009). For feature-based attention, unlike spatial attention, the model predicts only changes in response gain, regardless of whether the featural extent of the attention field is small or large. To test this prediction, we measured the contrast dependence of feature-based attention. Observers performed an orientation-discrimination task on a spatial array of grating patches. The spatial locations of the gratings were varied randomly so that observers could not attend to specific locations. Feature-based attention was manipulated with a 75% valid and 25% invalid pre-cue, and the featural extent of the attention field was manipulated by introducing uncertainty about the upcoming grating orientation. Performance accuracy was better for valid than for invalid pre-cues, consistent with a change in response gain, when the featural extent of the attention field was small (low uncertainty) or when it was large (high uncertainty) relative to the featural extent of the stimulus. These results for feature-based attention clearly differ from results of analogous experiments with spatial attention, yet both support key predictions of the normalization model of attention.

© 2012 Elsevier Ltd. All rights reserved.

### 1. Introduction

Covert attention, the selective processing of visual information in the absence of eye movements, improves behavioral performance. Most studies of attention have examined the effects of selectively attending at particular locations in the visual field. However, attention can also be selectively deployed to visual features, such as particular orientations, colors or directions of motion, regardless of their locations in the visual field. Feature-based attention (FBA) enhances particular features within a dimension at the expense of unattended or behaviorally irrelevant features. Thus, it is an important component for a visual system that needs to devote limited processing resources on the most relevant sensory inputs regardless of where in the visual field they are located. FBA enhances the representation of image components that share a particular feature throughout the visual field. FBA is important because we often know a defining feature of an object without knowing its location – e.g., your friend is somewhere in the cafeteria and she often wears a purple shirt.

FBA has been characterized in single-unit (e.g., Haenny, Maunsell, & Schiller, 1988; Martinez-Trujillo & Treue, 2004; Maunsell &

Treue, 2006; Motter, 1994a, 1994b; Treue & Martinez Trujillo, 1999), psychophysical (e.g., Alais & Blake, 1999; Baldassi & Verghese, 2005; Lankheet & Verstraten, 1995; Ling, Liu, & Carrasco, 2009; Liu, Stevens, & Carrasco, 2007; Spering & Carrasco, in press; Spivey & Spirn, 2000; White & Carrasco, 2011), and neuroimaging (e.g., Liu, Larsson, & Carrasco, 2007; Saenz, Buracas, & Boynton, 2002, 2003; Serences & Boynton, 2007; Serences et al., 2009) studies. For a review, see Carrasco (2011).

Activity in visual cortex increases with stimulus contrast (Boynton et al., 1999; Carandini, Heeger, & Movshon, 1997; Desimone & Schein, 1987; Heeger, 1992) and several models of attention have proposed that attention, both spatial and feature-based, may modulate the neural response amplitudes, producing an effect similar to changes in stimulus contrast (Boynton, 2009; Ghose, 2009; Lee & Maunsell, 2009; Reynolds & Heeger, 2009; Reynolds, Pasternak, & Desimone, 2000). Spatial attention has been shown to robustly modulate responses to stimulus contrast in behavioral (Carrasco, Penpeci-Talgar, & Eckstein, 2000; Herrmann et al., 2010; Ling & Carrasco, 2006; Lu & Doshier, 1998; Morrone, Denti, & Spinelli, 2002, 2004; Pestilli & Carrasco, 2005; Pestilli, Ling, & Carrasco, 2009; Pestilli, Viera, & Carrasco, 2007; Yigit-Elliott, Palmer, & Moore, 2011), single unit (Buracas & Boynton, 2007; Li et al., 2008; Martinez-Trujillo & Treue, 2002; McAdams & Reid, 2005; Reynolds & Chelazzi, 2004; Reynolds, Pasternak, & Desimone, 2000; Williford & Maunsell, 2006) and neuroimaging studies (Buracas & Boynton,

\* Corresponding author at: Department of Psychology, New York University, United States.

E-mail address: [marisa.carrasco@nyu.edu](mailto:marisa.carrasco@nyu.edu) (M. Carrasco).

2007; Liu, Pestilli, & Carrasco, 2005; Lu et al., 2011; Murray & He, 2006; Pestilli et al., 2011). Yet, neither behavioral nor neurophysiology studies have systematically characterized the contrast dependence of FBA. One neurophysiology study has reported that FBA varies with different stimulus contrasts (Khayat, Niebergall, & Martinez-Trujillo, 2010), but the task that was used does not fully exclude a spatial attention contribution (see Section 4).

The normalization model of attention was proposed to reconcile previous, seemingly contradictory findings on the effects of visual attention, to unify alternative models on attention, and to offer a computational framework to simulate new research questions (Carandini & Heeger, 2011; Reynolds & Heeger, 2009). Based on the model, FBA can be characterized with an attention field selective for a feature (such as orientation or direction of motion), but not selective (constant) across spatial positions (Fig. 1A). The attention field is multiplied with the stimulus drive, and then normalized, such that the extent of the stimulus and the relative extent of the attention field can shift the balance between excitation and

suppression. Thus, the model can exhibit different effects of attentional modulation, described in the literature, such as response gain changes that increase firing rates by a multiplicative scale factor without changing the shape or width of neuronal tuning (McAdams & Maunsell, 1999; Treue & Maunsell, 1999); contrast gain changes that increase responses, multiplying the stimulus contrast by a scale factor (Martinez-Trujillo & Treue, 2002; Reynolds, Pasternak, & Desimone, 2000); a combination of both response gain and contrast gain changes (Williford & Maunsell, 2006); or sharpening of neuronal tuning (Martinez-Trujillo & Treue, 2004; Spitzer, Desimone, & Moran, 1988).

The goal of the present study was to measure the contrast dependence of FBA in humans. We used the normalization model of attention (Reynolds & Heeger, 2009; Fig. 1A) to simulate possible outcomes, before conducting any experiments. According to this model, there are the two key parameters that determine the type of attentional gain modulation (response gain, contrast gain or a mixture of both): the extent of the stimulus and relative extent of the attention field. Experimental findings have supported the importance of these two parameters for the type of gain for spatial attention (Herrmann et al., 2010). For FBA, our simulations resulted in these two testable predictions: FBA improves performance accuracy consistent with a change in response gain both (1) when the featural extent of the attention field is small relative to the featural extent of the stimulus (Fig. 1B), and also (2) when the featural extent of the attention field is large relative to the featural extent of the stimulus (Fig. 1C). [The specifics of the model simulations are presented below.]

We empirically tested these two predictions of the normalization model of attention. Because a visual stimulus always occupies a certain spatial location, we controlled the spatial arrangement of the stimuli so that task performance would not benefit by attending to different locations across conditions or trials. Any measured benefits in performance therefore reflected specifically the impact of FBA. Stimuli contained two orientations, intermingled over the same spatial location around fixation, and stimulus contrast covaried for both orientations and varied unpredictably across trials.

To manipulate FBA, observers were cued to covertly attend to one of the two orientations and perform a fine orientation-discrimination task while fixating. We manipulated the featural extent of the attention field by introducing uncertainty about the upcoming stimulus orientations. This design allowed us to measure the contrast dependence of FBA, while spatial attention was distributed, i.e., not directed to any specific location. Control experiments verified that the uncertainty manipulation was effective; performance accuracy depended systematically and predictably on whether a single orientation was cued or a large range of orientations was cued. We found, as predicted by the model, that FBA enhanced performance consonant with a change in response gain, with low or high uncertainty about the upcoming orientation.

## 2. Experiments

### 2.1. Methods

Experiments were conducted with the written consent of each observer. The University Committee on Activities Involving Human Subjects at New York University approved the procedures.

### 2.2. Observers

Six observers (25–33-year-old; three females) with normal or corrected vision participated in the experiments. Four observers participated in each of the two main experiments: the

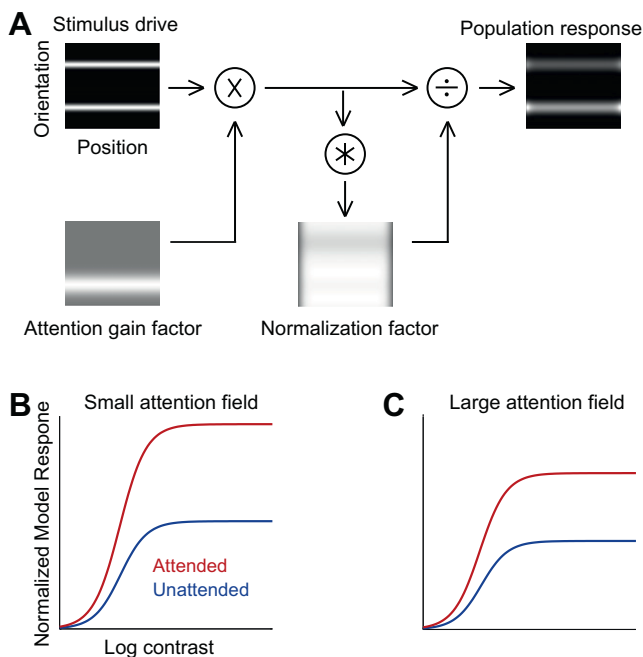


**Fig. 1.** Model and predictions. (A) Using the normalization model of attention (Reynolds & Heeger, 2009) to simulate FBA. Stimuli, presented as input to the model, were two spatially overlapping orientations identical in contrast, one of which was attended. The upper left panel depicts the stimulus drive for a population of neurons with various receptive field centers (horizontal) and orientation preferences (vertical). Brightness at each location in the image corresponds to the stimulus drive for a single neuron. Lower left panel shows the attention field when attending to the right-tilted orientation. Gray indicates a value of 1 and white indicates an attentional gain factor greater than 1. The attention field is multiplied point-by-point with the stimulus drive. Bottom right panel, the normalization factors are computed by the product of the stimulus drive and the attention field, and then pooled over space and orientation through convolution with the suppressive field. Right panel, neural image depicting the output firing rates of the population of simulated neurons, computed by dividing the stimulus drive by the normalization factors. The stimulus drive, attention field, and normalization factor all had Gaussian profiles in space and orientation. (B) Simulation results for small attention field, i.e., featural extent of the attention field small relative to featural extent of the stimulus. Red curve, contrast-response function for a simulated neuron when attending the neuron's preferred orientation. Blue curve, contrast-response function when attending the non-preferred orientation. (C) Simulation results for large attention field. Only the featural extent of the attention field was changed in the simulations; all other model parameters were identical in both panels. The model predicts a change in response gain (largest effects at higher contrasts, upward scaling of the contrast-response function) for both small and large attention fields.

low-uncertainty experiment and the high-uncertainty experiment. Three of them completed both experiments.

### 2.3. Apparatus

Visual stimuli were generated with an Apple Macintosh OS X (Intel Xeon) computer using MATLAB (The MathWorks, Natick, MA) and MGL (<http://gru.brain.riken.jp/doku.php>). Stimuli were displayed on a calibrated and linearized  $40 \times 30$  cm CRT monitor (HP P1230) with a refresh rate of 75 Hz and gray background luminance of  $37.6 \text{ cd/m}^2$ . An infrared-video eye-tracker (EyeLink 1000, SR Research Ltd., Mississauga, Ontario, Canada) was used to record eye position (right eye, 500 Hz). Observers viewed stimuli in a dark room on a chin rest at a distance of 57 cm.

### 2.4. Procedure

Observers participated in practice sessions to determine individual orientation-discrimination thresholds (JND, just noticeable difference), followed by four to six 1 h experimental sessions. This resulted in 13,838 trials (10,378 valid; 3460 invalid) in the low-uncertainty experiment and in 14,418 (10,815 valid; 3603 invalid) trials in the high-uncertainty experiment. In addition, there were two control experiments. Two observers completed the masking control experiment that consisted of six 1 h experimental sessions: observer 1 completed 4499 trials (3374 valid; 1125 invalid), observer 2 completed 4320 trials (3240 valid; 1080 invalid). Four observers participated in the uncertainty control experiment, which consisted of five 1 h experimental sessions, resulting in a total of 12,960 trials (9720 valid; 3240 invalid).

In all experiments, observers were instructed to maintain fixation throughout each trial. Eye position was measured to verify that observers kept their gaze at fixation. The eye tracker was calibrated at the beginning of each 12-min block.

### 2.5. Experimental protocols

#### 2.5.1. Low-uncertainty

Stimuli consisted of 32 sinusoidal grating (Gabor) patches ( $\sigma = 0.16^\circ$ , SD of Gaussian window; spatial frequency = 3.8 cycles per degree) arranged on a  $9^\circ \times 9^\circ$  regular grid centered at fixation. The central four out of 36 center positions were omitted, such that the innermost Gabors were centered  $2.7^\circ$  away from fixation. Positions of each Gabor were randomly and independently jittered (uniform distribution,  $0$ – $0.6^\circ$  of horizontal and vertical center grid positions) in each interval and trial. Doing so encouraged observers to distribute attention spatially throughout the display because the exact locations were uncertain and could not be predicted in advance. The stimulus displays were brief (150 ms).

Observers performed a fine orientation-discrimination task (Fig. 2A). In the first 150 ms stimulus display, a random selection of 16 (out of 32) Gabor stimuli had identical orientation  $\theta_R$  near  $45^\circ$  (right-tilted), and the other 16 had identical orientation  $\theta_L$  near  $-45^\circ$  (left-tilted), resulting in two spatially interleaved orientations. In the second 150 ms stimulus display, the 32 Gabors all shared identical orientation  $\theta_{\text{test}}$ , chosen randomly to be either near  $45^\circ$  or  $-45^\circ$  (Fig. 2B). The precise values of the orientations  $\theta_{\text{test}}$  ( $\pm 42^\circ$ ,  $45^\circ$  or  $48^\circ$ ),  $\theta_R$  ( $\theta_{\text{test}} \pm 1 \text{ JND}$ ) and  $\theta_L$  ( $\theta_{\text{test}} \pm 1 \text{ JND}$ ) were randomly and independently varied across trials so that the first stimulus display was uninformative as to which orientation would be queried. This small orientation jitter also allowed us to explore observers' strategy to perform the fine orientation discrimination task. Observers were asked to indicate whether the orientation  $\theta_{\text{test}}$  in stimulus display 2 was slightly clockwise or counter-clockwise of the closest orientation in stimulus display 1. Observers received auditory feedback if their response was incorrect. Contrasts of

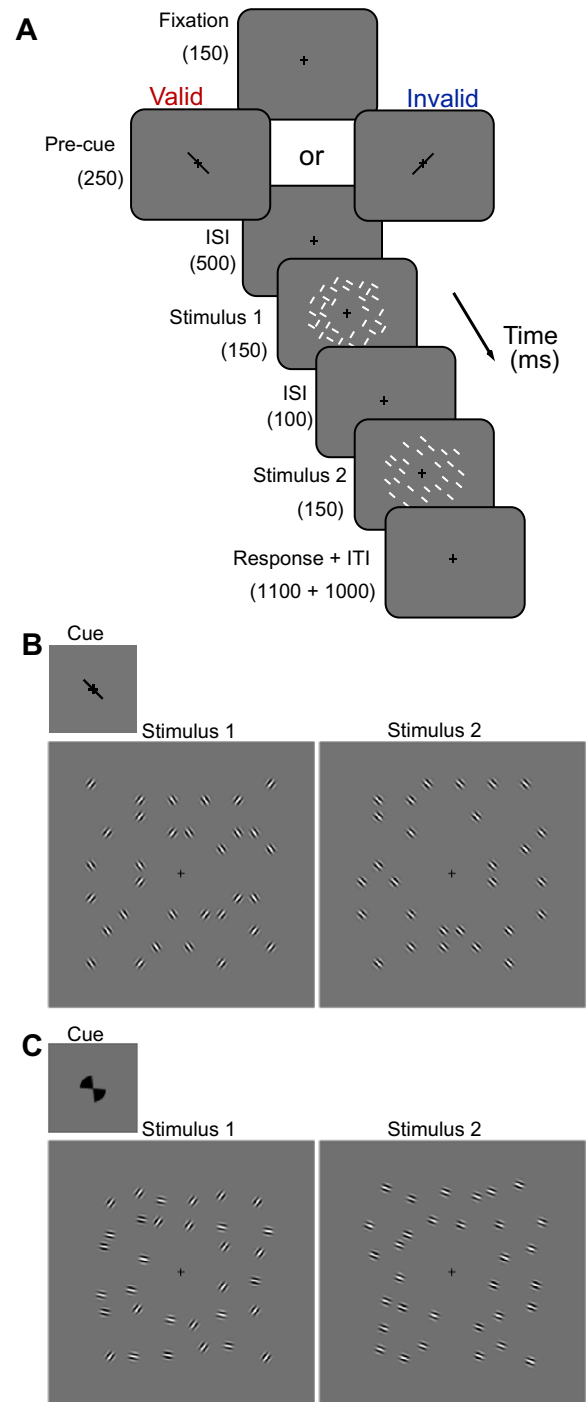


**Fig. 2.** Experimental protocol. (A and B) Feature-based attention (FBA) task. Observers performed an orientation discrimination task and reported whether the orientation in stimulus display 2 was slightly clockwise or counter-clockwise of the closest orientation in stimulus display 1. Stimulus 1 and 2 had the same contrast, which varied from trial to trial. ISI, interstimulus interval; ITI, intertrial interval. The white lines in both stimulus intervals indicate stimulus locations that were randomly jittered. (B) Stimulus displays in the low-uncertainty experiment. Top (inset), low-uncertainty cue, left or right tilted line. Left panel, stimulus 1 consisted of two spatially interleaved orientations around fixation. Right panel, stimulus 2 consisted of 32 grating patches with identical orientation, which was slightly clockwise or counter-clockwise of one of the orientations in stimulus 1. (C) High uncertainty experiment. High-uncertainty cue, left or right tilted segments. Stimulus displays, in the high-uncertainty experiment. Same format as panel B. Stimulus 1, the right-tilted orientation could be one of 21 possible orientations between  $15^\circ$  and  $75^\circ$ ; the left-tilted orientation could also be one of 21 possible orientations between  $-15^\circ$  and  $-75^\circ$ . The two orientations varied randomly and independently, with the constraint that they were at least  $60^\circ$  apart. Stimulus 2 was slightly clockwise or counter-clockwise of one of the orientations in stimulus 1.

Gabor stimuli in the first and second interval were identical, but varied from trial to trial in a randomly shuffled order. There were nine contrasts, equally separated on a logarithmic scale (5%, 7.12%, 10.15%, 14.47%, 20.62%, 29.38%, 41.86%, 59.65%, and 85%). The mean JND across observers was  $3.7^\circ$ , SEM =  $0.16^\circ$  (O1:  $3.47^\circ \pm 0.25^\circ$ ; O2:  $3.65^\circ \pm 0.37^\circ$ ; O3:  $3.5^\circ \pm 0.29^\circ$ ; O4:  $4.17^\circ \pm 0.21^\circ$  (mean  $\pm$  SD across contrasts)).

FBA was manipulated with a pre-cue (Fig. 2B). The pre-cue was a  $1.2^\circ$  green line at fixation, oriented either  $45^\circ$  or  $-45^\circ$  in random order from trial to trial, presented for 250 ms. A 500 ms cue-stimulus onset asynchrony allowed sufficient time for covert FBA to be deployed (Liu, Stevens, & Carrasco, 2007). Target orientation in stimulus display 1 was indicated by a similar orientation  $\theta_{\text{test}}$  in stimulus display 2. A valid pre-cue was defined as a ‘match’ between pre-cue orientation and the orientation in stimulus display 2 (75% of the trials); a ‘mismatch’ yielded an invalid pre-cue (25% of the trials). The order of valid and invalid pre-cues was randomly shuffled. The cued orientation was randomly drawn from an equal distribution on each trial. Observers were explicitly told that the pre-cued orientation was informative and that using the pre-cue orientation would improve their task performance.

### 2.5.2. High-uncertainty

The protocol was identical to the one in the low-uncertainty experiment (Fig. 2A), except for the following: (1) The pre-cue was a  $60^\circ$ -segment, indicating the wide range of possible upcoming orientations (Fig. 2C), rather than a line indicating upcoming orientations of very near  $\pm 45^\circ$ . (2) Stimulus orientations varied over a wide range:  $\theta_{\text{test}}$  ( $\pm 15$ – $75^\circ$ , in steps of  $3^\circ$ , resulting in 21 possible left-tilted orientations and 21 possible right-tilted orientations),  $\theta_R$  ( $\theta_{\text{test}} \pm 1$  JND) and  $\theta_L$  ( $\theta_{\text{test}} \pm 1$  JND). The precise values of the two orientations  $\theta_R$  and  $\theta_L$  varied randomly (according to a uniform distribution) and independently over trials, with the constraint that they were at least  $60^\circ$  apart. The range of possible orientations was about six times larger than in the low-uncertainty experiment. The mean JND across observers was  $5.06^\circ$ , SEM =  $0.52^\circ$  (O1:  $4.51^\circ \pm 0.17^\circ$ ; O2:  $4.68^\circ \pm 0.21^\circ$ ; O3:  $4.44^\circ \pm 0.18^\circ$ ; O4:  $6.59^\circ \pm 0.67^\circ$  (mean  $\pm$  SD across contrasts)).

Task difficulty was adjusted separately for each individual observer, and separately for the low- and high-uncertainty experiments. Specifically, the orientation difference between the two stimulus displays was selected based on pilot experiments. The protocol in these experiments was identical to that in the main experiments except that the contrast was fixed at 85% and the pre-cue was neutral. The neutral pre-cue for the low-uncertainty experiment was composed of two overlapping lines ( $+45^\circ$  and  $-45^\circ$ ; Fig. 2B) at fixation, and it was composed of two overlapping segments at fixation in the high-uncertainty experiment (Fig. 2C). The orientation difference was adjusted, using a staircase procedure (Watson & Pelli, 1983) to determine individual tilt thresholds ( $\sim 75\%$  correct).

### 2.5.3. Masking control

The protocol was identical to the low-uncertainty experiment, except that the locations of the Gabor stimuli were spatially randomized with the constraint that they would never spatially overlap between the two stimulus displays. A  $10.4^\circ \times 10.4^\circ$ -stimulus grid with 128 pre-defined stimulus locations was used, omitting the central  $2.4^\circ$ . In stimulus display 1, 32 of the pre-defined locations were randomly chosen, half of them randomly displaying the target orientation and the other half displaying the distracter orientation. In stimulus display 2, 32 Gabor stimuli were presented at a random selection of the 96 remaining locations. Doing so ensured that observers could not attend spatially just one or two locations. In addition, the contrast of stimulus display 2 had a constant value of 20.62% in all trials to determine if differential

masking, as a function of contrast, between the two stimulus displays might have confounded the interpretation of the results.

### 2.5.4. Uncertainty control

To verify that observers used the uncertainty pre-cue, the low- and high-uncertainty experiments were repeated with the same orientation difference  $\Delta\theta$  in the orientation discrimination task ( $\Delta\theta = |\theta_L - \theta_{\text{test}}|$ , where  $|\theta_L - \theta_{\text{test}}| = |\theta_R - \theta_{\text{test}}|$ ). The orientation difference  $\Delta\theta$  was fixed for each observer (O1:  $3^\circ$ ; O2, O3, and O4:  $4.5^\circ$ ) such that the two uncertainty conditions could be directly compared. Low- and high-uncertainty blocks were alternated within each experimental session; the order was counter-balanced across observers. Stimuli were displayed at one contrast (85%) only.

## 2.6. Data analysis

### 2.6.1. Psychophysics

Performance,  $d' = z(\text{hit rate}) - z(\text{false alarm rate})$ , was computed for each observer across experimental sessions, separately for each contrast and each pre-cue (valid and invalid) (see also Herrmann et al., 2010). A hit was (arbitrarily) defined as counter-clockwise response to counter-clockwise stimulus tilt and a false alarm as counter-clockwise response to clockwise stimulus. The psychometric data were fit with the Naka–Rushton equation (e.g., Ross and Speed, 1991) to the mean performance (across observers), using a nonlinear least-square procedure:

$$d'(c) = d'_{\text{max}} \frac{c^n}{c^n + c_{50}^n}$$

where  $d'(c)$  is performance as a function of contrast,  $d'_{\text{max}}$  is the asymptotic performance at high contrasts,  $c_{50}$  is the contrast corresponding to half the asymptotic performance and  $n$  is an exponent that controls the slope of the psychometric function. The two parameters  $d'_{\text{max}}$  and  $c_{50}$  determined response gain and contrast gain, respectively. These two parameters were estimated for each attention condition (valid and invalid). The exponent was estimated as a single free parameter, constrained to have the same value for both attentional conditions.

The 68% confidence intervals for the fitted response gain ( $d'_{\text{max}}$ ) and contrast gain ( $c_{50}$ ) parameters were estimated using a bootstrap procedure (Fig. 3). This bootstrap procedure was used to assess whether changes in response gain and/or contrast gain were statistically significant. Specifically, individual psychophysical trials were randomly resampled with replacement. The resampled data set was refit. This procedure of resampling and refitting was repeated 10,000 times, which resulted in bootstrap distributions of the psychometric data and of the fitted parameters. We assembled the bootstrap distribution of the differences between the conditions (valid versus invalid trials) and performed statistical tests by assessing the percentage of the values in the tail of the distribution of the differences greater than zero for response gain changes ( $d'_{\text{max}}$ ), or less than zero for contrast gain changes ( $c_{50}$ ).

### 2.6.2. Eye movements

Raw data were converted to eye position in degrees of visual angle. Eye position during the fixation interval at the beginning of each trial served as baseline and was subtracted from eye position during the stimulus interval, to compensate for any slow drift in the measurements/calibration during each block. A standard EyeLink detection algorithm (velocity threshold =  $30^\circ/\text{s}$ , and acceleration threshold =  $8000^\circ/\text{s}^2$ ) was used to detect saccades, and the percentage of trials in which saccades occurred were counted. The EyeLink software was used to detect blinks, and the time points shortly (100 ms) preceding and following blinks were excluded from

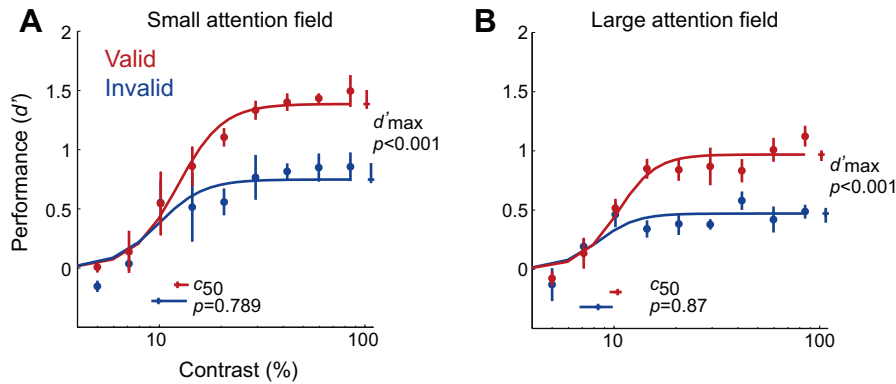


**Fig. 3.** Psychometric functions. (A) Small attention field, (low-uncertainty). (B) Large attention field (high-uncertainty). Each panel plots performance accuracy ( $d'$ ) as a function of contrast, for valid (red) and invalid (blue) pre-cues. Each data point represents the mean across observers. Error bars on data points are  $\pm 1$  s.e.m. ( $n = 4$  observers). Curves, best-fit of the Naka–Rushton equation yielding parameter estimates  $c_{50}$  (contrast yielding half-maximum performance) and  $d'_{\max}$  (asymptotic performance at high contrast). Error bars on parameter estimates are 68%-confidence intervals, obtained by bootstrapping.

analysis. The first two trials of each block were ignored. For statistical analysis (two-tailed  $t$ -tests), trials were sorted according to pre-cue orientations (left- or right-tilt) and compared for horizontal and vertical deviations from the center. Deviations from the center (horizontal and vertical) were also compared in the high- and low-uncertainty conditions.

### 3. Results

#### 3.1. Model simulations

For simulations, we used the normalization model of attention (Reynolds & Heeger, 2009). The matlab code is available online ([http://www.snl-r.salk.edu/~reynolds/Normalization\\_Model\\_of\\_Attention/](http://www.snl-r.salk.edu/~reynolds/Normalization_Model_of_Attention/) or <http://www.cns.nyu.edu/heegerlab>).

The relative stimuli and attention fields varied across two simulations: (1) the featural extent of the attention field was small relative to the feature extent of the stimulus ( $5^\circ$  versus  $10^\circ$ ) (Fig. 1B), (2) the featural extent of the attention field was large relative to the feature extent of the stimulus ( $30^\circ$  versus  $10^\circ$ ) (Fig. 1C). The featural extent of the attention field corresponds to the range of pre-cued orientations (relative to standard deviation of the featural extent of the stimulus). The featural extent of the stimulus corresponds to the standard deviation of the bandwidth at half amplitude of the Gabors. Specifically, we computed the 2-dimensional Fourier transform of one array of Gabors (16 locations; stimulus contrast: 85%) and computed the orientation-bandwidth at half maximum amplitude. We repeated this procedure for a random sampling of stimulus arrays, resulting in a distribution of full-width half-height values. Finally, we computed the median value of the distribution.

All other model parameters were identical in both simulations. In the feature domain, we set the orientation bandwidth of the stimulation field to  $17^\circ$ . This value corresponds to the bandwidth at half amplitude of  $40^\circ$  for V4 (De Valois, Yund, & Hepler, 1982; Desimone & Schein, 1987; McAdams & Maunsell, 1999). We used a broad tuning width of the suppressive field of  $180^\circ$  (or set it to be constant). Orientation tuning curves were Gaussian functions; tuning widths were in degrees corresponding to the standard deviation of the Gaussian. In the spatial domain, the size of the stimulation field was set to  $5^\circ$  in visual angles, corresponding to the receptive field size of neurons in V4 at eccentricity of  $5^\circ$  (Cavanaugh, Bair, & Movshon, 2002a, 2002b; Dumoulin & Wandell, 2008). The eccentricity of  $5^\circ$  corresponds to half the stimulus length from center used in the two experiments. The size of the

suppressive field was set to  $20^\circ$ , which is four times the stimulation field (Reynolds & Heeger, 2009). We simulated the spatial extent of the large stimulus as being constant. To simulate distributed spatial attention across the visual field, the size of the spatial attention field was set to be equal to the size of the extent of the stimulus. The qualitative results of the simulation (response gain) were robust to the simulation parameters, even when doubling or halving the featural attention field sizes or stimulus bandwidth values.

The simulations resulted in two testable predictions: FBA should improve performance accuracy via a change in response gain both (1) when the featural extent of the attention field is small relative to the featural extent of the stimulus (Fig. 1B; compare also Fig. 4D and E of Reynolds and Heeger (2009) for direction of motion), and (2) when the attention field is large relative to the featural extent of the stimulus (Fig. 1C). The latter simulation predicted a change in contrast gain only when the orientation bandwidth of the stimulation field was set to be unrealistically narrow (e.g.,  $3^\circ$ ).

#### 3.2. High and low featural-uncertainty

Comparing performance accuracy ( $d'$ ) for valid and invalid trials revealed differences in behavioral performance. Accuracy improved with FBA, consistent with changes in response gain. When uncertainty was minimal, attention increased asymptotic performance at high contrasts (Fig 3A): there were robust differences in  $d'_{\max}$  (valid:  $d'_{\max} = 1.39$ , 68% confidence interval = [1.35, 1.50]; invalid:  $d'_{\max} = 0.75$ , 68% confidence interval = [0.72, 0.89];  $p < 0.001$ ), but there was no evidence for a change in  $c_{50}$  (valid:  $c_{50} = 0.12$ , 68% confidence interval = [0.12, 0.14]; invalid:  $c_{50} = 0.10$ , 68% confidence interval = [0.09, 0.13],  $p = 0.79$ ). The quality of the fit was  $R^2 = 0.95$ .

When uncertainty was high (Fig 3B), attention also increased asymptotic performance at high contrasts: there were robust differences in  $d'_{\max}$  (valid:  $d'_{\max} = 0.97$ , 68% confidence interval = [0.92, 1.01]; invalid:  $d'_{\max} = 0.47$ , 68% confidence interval = [0.39, 0.52];  $p < 0.001$ ), but no evidence for a change in  $c_{50}$  (valid:  $c_{50} = 0.10$ , 68% confidence interval = [0.10, 0.11]; invalid:  $c_{50} = 0.08$ , 68% confidence interval = [0.07, 0.10],  $p = 0.87$ ). The quality of the fit was  $R^2 = 0.90$ .

We constrained the exponent  $n$  to have the same value for all conditions in the low and high featural-uncertainty experiments and obtained a best-fit value of  $n = 4.39$  (68% confidence interval = [3.18, 5.47]). Refitting the data, allowing the exponent to vary independently for each experiment, also yielded the same conclusion: a change in response gain, both with low and high

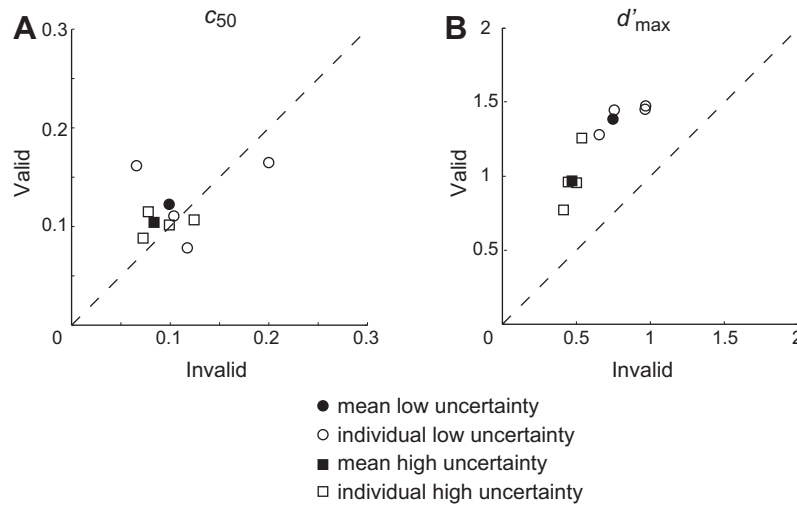


**Fig. 4.** Parameter estimates for individual observers. (A) Contrast yielding half-maximum performance  $c_{50}$ . Circles, small attention field (low uncertainty). Squares, large attention field (high uncertainty). Open symbols, individual observers. Filled symbols, mean across observers. (B) Asymptotic performance at high contrasts  $d'_{\max}$ . Same format as panel A.

featural-uncertainty. Best-fitting values for the exponents of the psychometric functions were similar for the low-uncertainty ( $n = 3.98\%$ , 68% confidence interval = [2.67, 5.04]) and high-uncertainty ( $n = 4.72\%$ , 68% confidence interval = [3.78, 10.483]) experiments.

The same results were evident in the behavioral performance of all individual observers (Fig. 4). For the individual observer analysis, the  $d'$  performance across experimental sessions was computed separately for each condition and contrast. We fit psychometric functions (see above) to estimate  $c_{50}$  (Fig. 4a), and  $d'_{\max}$  (Fig. 4b) for each observer. Small attention fields (relative to the stimulus extent) yielded similar  $c_{50}$  values for valid and invalid pre-cues (one-tailed paired  $t$ -test,  $p = 0.63$ ; one-tailed Wilcoxon,  $p = 0.38$ ), and reliably resulted in larger  $d'_{\max}$  values for valid than for invalid pre-cues (one-tailed  $t$ -test,  $p < 0.001$ ; one-tailed Wilcoxon,  $p < 0.001$ ). Similarly, large attention fields consistently resulted in similar  $c_{50}$  values for the two pre-cue conditions (one-tailed  $t$ -test,  $p = 0.88$ ; one-tailed Wilcoxon,  $p = 0.13$ ), but resulted in larger  $d'_{\max}$  values for valid than invalid pre-cues (one-tailed  $t$ -test,  $p < 0.001$ ; one-tailed Wilcoxon,  $p < 0.001$ ).

### 3.3. Masking control experiment

Masking did not confound the interpretation of our results. We replicated the results of the low-uncertainty experiment in two observers, using a variation of the protocol in which: (1) the stimuli were restricted to never even partially overlap between stimulus displays 1 and 2, and (2) the stimulus contrast of display 1 varied, while display 2 had a constant stimulus contrast of 20.62%, which was high relative to the mean  $c_{50}$ . FBA again resulted in a change in performance consistent with a change in response gain. While there was no evidence for a change in  $c_{50}$  (O1: valid:  $c_{50} = 0.10$ , CI = [0.10; 0.11]; invalid:  $c_{50} = 0.10$ ; CI = [0.10; 0.15];  $p = 0.50$ ; O2: valid:  $c_{50} = 0.09$ , CI = [0.08; 0.10]; invalid:  $c_{50} = 0.10$ , CI = [0.09; 0.13];  $p = 0.18$ ), there were robust differences in  $d'_{\max}$  between valid and invalid pre-cues (O1: valid:  $d'_{\max} = 1.53$ , CI = [1.51; 1.67]; invalid:  $d'_{\max} = 0.59$ , CI = [0.48; 0.75];  $p < 0.001$ ; O2: valid:  $d'_{\max} = 1.19$ , CI = [1.11; 1.28]; invalid:  $d'_{\max} = 0.90$ , CI = [0.73; 1.01];  $p = 0.02$ ).

### 3.4. Uncertainty control experiment

The uncertainty control experiment included both high- and low-uncertainty conditions within the same experimental session.

We compared performance in trials with identical stimuli by selecting from the high-uncertainty experiment the subset of trials in which the stimulus orientations were the same as those in the low-uncertainty experiment. Performance ( $d'$ ) was averaged across observers, separately for valid and invalid pre-cues, and separately for the high-uncertainty and the low-uncertainty conditions (Fig. 5). We analyzed only the common orientations:  $\theta_{\text{test}}$  of  $\pm 42^\circ$ ,  $45^\circ$  or  $48^\circ$ ,  $\theta_R$ :  $\theta_{\text{test}} \pm 1$  JND and  $\theta_L$ :  $\theta_{\text{test}} \pm 1$  JND. Thus, only the uncertainty (the shape of the pre-cue) was different between the two conditions, either directing observer's attention only to orientations near  $\pm 45^\circ$  or to a larger orientation range centered on  $\pm 45^\circ$ . This analysis included 6480 trials (4860 valid; 1620 invalid) per observer in the low-uncertainty condition and 1100 trials ( $\sim 825$  valid;  $\sim 275$  invalid) per observer in the high-uncertainty condition.

Mean performance with high-uncertainty was worse than with low-uncertainty. For valid pre-cues, observers performed significantly worse in the high- compared to the low-uncertainty condition (one-tailed paired  $t$ -test,  $p = 0.013$ ; one-tailed Wilcoxon,  $p = 0.014$ ), indicating that observers focused their attention in the low-uncertainty condition and spread their attention in the high-uncertainty condition. All observers showed a similar pattern of results. Our hypothesis concerned the valid pre-cue trials, but there was a non-significant trend in the same direction for invalid

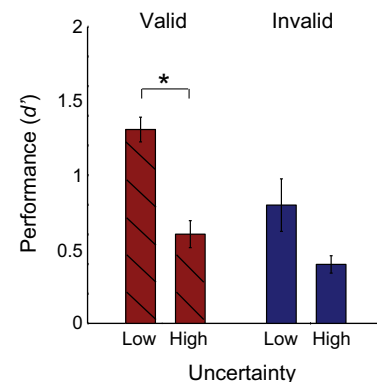


**Fig. 5.** Uncertainty control experiment. Performance as a function of uncertainty for valid pre-cues. Each bar represents the mean across observers, for trials with the same orientations in high- and low-uncertainty blocks. Error bars,  $\pm 1$  s.e.m. ( $n = 4$  observers). \* $p < 0.05$ , one-tailed  $t$ -test, Wilcoxon test.

pre-cues (two-tailed paired *t*-test,  $p = 0.075$ , two-tailed Wilcoxon,  $p = 0.200$ ).

Similar results were obtained when all orientations (all trials) of the high-uncertainty condition were included in the analysis. Observers performed better in the low-uncertainty than in the high-uncertainty condition (valid low-uncertainty versus valid high-uncertainty: one-tailed paired *t*-test,  $p = 0.004$ , one-tailed Wilcoxon,  $p = 0.014$ ; invalid low-uncertainty versus invalid high-uncertainty: two-tailed *t*-test,  $p = 0.101$ ; two-tailed Wilcoxon,  $p = 0.200$ ).

### 3.5. Spread of feature-based attention

We reanalyzed the data to evaluate whether observers spread FBA across the range of possible orientations in the high-uncertainty experiment (Fig. 6). Specifically, performance (averaged across four observers and nine contrasts) in valid (Fig. 6A, red bars) and invalid trials (Fig. 6A, blue bars) was analyzed for different orientation ranges in which the full orientation range of  $\theta_{\text{test}} (\pm 15^\circ - 75^\circ)$  was sub-divided into five bins of  $9^\circ$  each.

The difference in performance between valid and invalid trials in each orientation bin did not differ from the mean differential performance of all other bins (two-tailed paired *t*-tests and Wilcoxon, all comparisons  $p > 0.1$ ). In addition, to test whether attention improved performance, we subtracted performance of invalid from valid trials. The differential performance of each orientation sub-range was significantly larger than zero (one-tailed *t*-tests, all comparisons  $p < 0.05$ , except for one, 15–24°).

In the low-uncertainty experiment, the pre-cue line was always  $+45^\circ$  or  $-45^\circ$  oriented. We introduced a small jitter near  $45^\circ$  in the orientation of stimulus 1 so that the stimulus display was uninformative by itself and observers had to wait for stimulus display 2 to perform the discrimination task. This small orientation jitter also allowed us to explore observers' strategy to perform the fine orientation discrimination task. In a post hoc analysis, we binned trials based on the orientation of stimulus 1 (Fig. 6B). The first bin included trials for which the orientation of stimulus 1 was closest to  $\pm 45^\circ$  ('45'). This occurred for the following four pairs of stimulus orientations: ( $\theta_{\text{test}} = 42^\circ$ ,  $\theta_R = \theta_{\text{test}} + 1 \text{ JND}$ ), ( $\theta_{\text{test}} = 48^\circ$ ,  $\theta_R = \theta_{\text{test}} - 1 \text{ JND}$ ), ( $\theta_{\text{test}} = -42^\circ$ ,  $\theta_L = \theta_{\text{test}} - 1 \text{ JND}$ ), ( $\theta_{\text{test}} = -48^\circ$ ,  $\theta_L = \theta_{\text{test}} + 1 \text{ JND}$ ). The second bin included trials for which the orientation of stimulus 1 was slightly more different from  $\pm 45^\circ$  ('near  $45^\circ$ ):  $\theta_{\text{test}} = \pm 45^\circ$  and  $\theta_R$  or  $\theta_L = \theta_{\text{test}} \pm 1 \text{ JND}$ . The third bin included the remainder of the trials for which the orientation of stimulus 1 was furthest from  $\pm 45^\circ$  ('far  $45^\circ$ '). This occurred for the following

four pairs of stimulus orientations: ( $\theta_{\text{test}} = 42^\circ$ ,  $\theta_R = \theta_{\text{test}} - 1 \text{ JND}$ ), ( $\theta_{\text{test}} = 48^\circ$ ,  $\theta_R = \theta_{\text{test}} + 1 \text{ JND}$ ), ( $\theta_{\text{test}} = -42^\circ$ ,  $\theta_L = \theta_{\text{test}} + 1 \text{ JND}$ ), ( $\theta_{\text{test}} = -48^\circ$ ,  $\theta_L = \theta_{\text{test}} - 1 \text{ JND}$ ).

Performance across the three bins was compared with two-tailed tests. Performance was best when stimulus 1 orientations were furthest from  $\pm 45^\circ$ , lower when stimulus 1 orientations were near  $\pm 45^\circ$ , and lowest when approximately equal to  $\pm 45^\circ$  ( $\pm 45^\circ$  versus far: *t*-test,  $p = 0.001$ ; Wilcoxon:  $p = 0.029$ ; far versus near: *t*-test,  $p = 0.009$ ; Wilcoxon:  $p = 0.057$ ; near versus  $\pm 45^\circ$ : *t*-test,  $p < 0.001$ ; Wilcoxon:  $p = 0.029$ ). This difference in performance as a function of stimulus orientation was evident for both valid and invalid pre-cues (Fig. 6B, red and blue bars, respectively; Table 1). Subtracting performance of invalid from valid trials revealed no evidence that the differential performances varied as a function of stimulus orientation (*t*-tests and Wilcoxon, all comparisons  $p > 0.1$ ; Table 1).

### 3.6. Eye positions

#### 3.6.1. Main experiment

Fixation was stable during stimulus presentation in the low- and high- uncertainty experiments. Saccades were detected in 0.96% and 0.67% of the trials in the low- and high-uncertainty experiments, respectively. The recorded gaze positions of all observers had a standard deviation of  $0.63^\circ$  horizontally and  $0.84^\circ$  vertically in the low uncertainty experiment, and  $1.18^\circ$  horizontally and  $2.04^\circ$  vertically in the high uncertainty experiment. The higher standard deviation in the high uncertainty experiment stems from one observer (low uncertainty experiment:  $1.00^\circ$  horizontally and  $0.97^\circ$  vertically; high uncertainty experiment:  $2.00^\circ$  horizontally and  $3.46^\circ$  vertically). All other observers had standard deviations  $< 0.45^\circ$  horizontally and  $< 1.27^\circ$  vertically in both experiments.

For left-tilted and right-tilted pre-cues, vertical gaze position distributions were statistically indistinguishable (two-tailed *t*-test comparison,  $p = 0.960$ ). Horizontal gaze positions differed ( $p < 0.001$ ; Bonferroni critical level = 0.0125), but the effect size was negligible (Cohen's effect size = 0.094; left-tilted pre-cues:  $M = 0.02^\circ$ ,  $SD = 0.48^\circ$  and right-tilted pre-cues:  $M = 0.11^\circ$ ,  $SD = 1.30^\circ$ ).

For the high- and low-uncertainty experiments, horizontal gaze positions were statistically indistinguishable ( $p = 0.364$ ). Vertical gaze position distributions differed ( $p = 0.009$ ), but the effect size was negligible (Cohen's effect size = 0.012; low uncertainty:  $M = 0^\circ$ ,  $SD = 0.84^\circ$  and high uncertainty:  $M = -0.06^\circ$ ,  $SD = 2.04^\circ$ ).

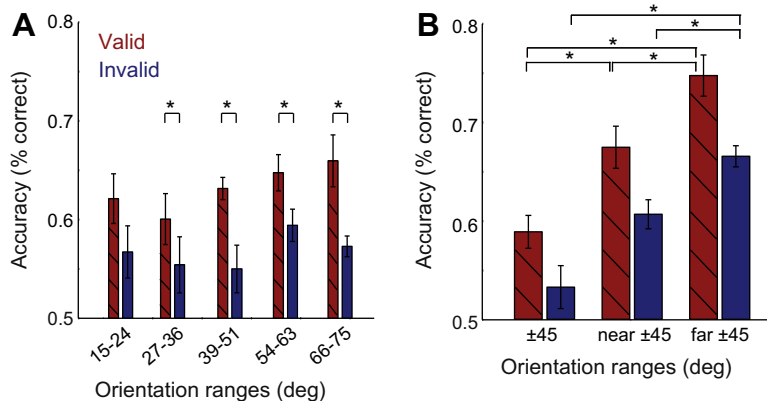


**Fig. 6.** Performance as a function of stimulus orientation. (A) Large attention field (high uncertainty). Each bar represents performance for a different range of stimulus orientations. Red, valid pre-cues. Blue, invalid pre-cues. Error bars,  $\pm 1$  s.e.m. ( $n = 4$  observers). Similar performance for all orientations indicated that observers spread their attention across orientations. (B) Small attention field (Low-uncertainty). Performance corresponding to each of three orientation ranges, combining right- and left-tilted orientations. Red, valid pre-cues. Blue, invalid pre-cues. Error bars,  $\pm 1$  s.e.m. ( $n = 4$  observers). \* $p < 0.05$ , *t*-tests, Wilcoxon test. (For interpretation of the references to color in this figure legend, the reader is referred to the web version of this article.)

**Table 1**Feature-based attention in the low-uncertainty experiment ( $n = 4$  observers).  $p$ -Values of two-tailed paired  $t$ -tests, and  $p$ -values of Wilcoxon tests in parenthesis.

Comparison of orientation ranges	Performance for $\pm 45^\circ$ < performance for near $\pm 45^\circ$	Performance for near $\pm 45^\circ$ < performance for far $\pm 45^\circ$	Performance for $\pm 45^\circ$ < performance for far $\pm 45^\circ$
Valid pre-cues	0.010 (0.057)	0.013 (0.057)	0.003 (0.029)
Invalid pre-cues	0.089 (0.057)	0.017 (0.029)	0.009 (0.029)
Valid minus invalid	0.804 (0.486)	0.500 (0.886)	0.467 (0.486)

### 3.6.2. Masking control experiment

Fixation was stable during stimulus presentation in this control experiment. Saccades were detected in 0.37% of the trials. The recorded gaze positions had a standard deviation of  $1.48^\circ$  horizontally and  $1.43^\circ$  vertically. There was no evidence that left-tilted and right-tilted pre-cues resulted in significantly different distributions (horizontal:  $p = 0.093$ . vertical:  $p = 0.177$ ).

### 3.6.3. Uncertainty control experiment

Fixation was stable during stimulus presentation in the low- and high-uncertainty control experiments. Saccades were detected in 0.91% and 0.50% of the trials in the low and high uncertainty blocks, respectively. The recorded gaze positions of all observers had a standard deviation of  $0.73^\circ$  horizontally and  $0.40^\circ$  vertically in the low-uncertainty experiment, and  $0.37^\circ$  horizontally and  $0.46^\circ$  vertically in the high-uncertainty experiment.

For left-tilted and right-tilted pre-cues, vertical gaze position distributions were statistically indistinguishable ( $p = 0.183$ ). Horizontal gaze positions differed ( $p < 0.001$ ), but the effect size was negligible (Cohen's effect size = 0.08; left-tilted pre-cues:  $M = 0.04^\circ$ ,  $SD = 0.73^\circ$  and right-tilted pre-cues:  $M = 0.09^\circ$ ,  $SD = 0.36^\circ$ ).

For the high- and low-uncertainty experiments, horizontal gaze positions were statistically indistinguishable ( $p = 0.292$ ). Vertical gaze position distributions differed ( $p = 0.001$ ), but the effect size was negligible (Cohen's effect size = 0.061; low uncertainty:  $M = 0.002^\circ$ ,  $SD = 0.40^\circ$  and high uncertainty:  $M = -0.025^\circ$ ,  $SD = 0.46^\circ$ ).

## 4. Discussion

FBA improved performance accuracy via a change in response gain, and not in contrast gain, both when the featural extent of the attention field was small (Figs. 3A and 4) and when it was large (Figs. 3B and 4) relative to the featural extent of the stimulus. In two experiments (Fig. 2) observers were cued to attend to one of two spatially superimposed orientations. In the low uncertainty experiment, the stimuli were selected from a narrow range of orientations. In the high uncertainty experiment, the two overlapping orientations were each chosen from a broad range of possible orientations. We verified that the uncertainty manipulation about the upcoming orientation was effective (Fig. 5) and that the spread of attention was less selective and wider for high- than low-uncertainty (Fig. 6).

The experimental design maximized the effects of FBA, while spatial attention was controlled and distributed. Target and distracter orientations were intermixed within the same space around fixation to keep the distribution of spatial attention the same for valid and invalid pre-cues. Observers were instructed to covertly attend to as many grating patches as possible, all sharing the same orientation close to the cued orientation, while ignoring the rest of the intermixed stimulus patches, all sharing a very different, uncued and behaviorally irrelevant orientation. Previous research has provided evidence that observers are able to perceptually group and average orientation signals to process them (Ben-Av & Sagi, 1995; Carrasco & Chang, 1995; Gheri & Baldassi, 2008; Parkes et al., 2001). To encourage observers to distribute their spatial

attention, we introduced spatial uncertainty by randomizing the locations of the stimulus patches within each stimulus display in each trial. Thus, attending to a single, small location in the visual field (or to just a few locations) would have harmed observer's performance, because either a target or a distractor or no stimulus at all might have been displayed at the attended location(s).

Backward masking cannot explain our findings. We minimized potential masking effects in our main experiments. The two displays were separated by a 100 ms blank interval, which is long enough to minimize masking given the spatial frequency and range of eccentricities of the stimuli (Adam et al., 1993; Breitmeyer & Ogmen, 2000; Gorea, 1987; Joffe & Scialfa, 1995; Rogowitz, 1983). Moreover, the stimuli were randomly distributed around fixation, such that they rarely spatially overlapped between displays 1 and 2, and stimulus displays 1 and 2 had equal contrast in each trial. Hence, had there been any masking, it would have been equal for all conditions (valid versus invalid, low-uncertainty versus high-uncertainty). Nonetheless, we performed a control experiment to ensure that stimuli never spatially overlapped and that the contrast of the second stimulus display was constant. Psychometric fits were again consonant with a change in response gain, consistent with the results in the main experiments.

### 4.1. Testing the normalization model of attention

We used the normalization model of attention (Reynolds & Heeger, 2009) to simulate the contrast dependence of FBA (Fig. 1A–C). The featural extent of the attention field is related to the feature bias in the biased competition model and to the “feature-similarity gain principle” (Boynton, 2005; Khayat, Niebergall, & Martinez-Trujillo, 2010; Martinez-Trujillo & Treue, 2004; Treue & Martinez Trujillo, 1999). The attention field in the normalization model of attention, however, does not directly alter firing rate by a scaling factor, but is instead mediated through normalization (Heeger, 1992; Reynolds & Heeger, 2009).

The model simulated neuronal contrast-response functions; here we used it to make predictions about the psychophysical data obtained in our experiments. How do the model predictions for performance relate to predictions for firing rates? Discrimination can be linked with neuronal responses, by incorporating a model of the noise or variability in neuronal responses, and by incorporating a decision rule (see also Herrmann et al., 2010). The noise in single-unit firing rates is Poisson-like, i.e. the variance increases with mean firing rates (Dean, 1981; Geisler & Albrecht, 1997; Shadlen & Newsome, 1998). However, after pooling signals across many neurons, it is likely that only the correlated noise remains (Averbeck, Latham, & Pouget, 2006), which might behave more like additive noise. In fact, psychophysical data suggest that perceptual performance is limited by an additive noise component, independent and identically distributed (IID) across trials (Katkov, Tsodyks, & Sagi, 2007). Once the IID noise model and a maximum-likelihood decision rule have been adopted, behavioral performance can be predicted from the pooled neuronal activity (Barlow et al., 1987; Geisler & Albrecht, 1997; Gold & Shadlen, 2001, 2007; Jazayeri & Movshon, 2006; Pestilli, Ling, & Carrasco, 2009; Shadlen et al., 1996). Performance accuracy,  $d'$ , is then proportional to the signal-to-noise ratio of the underlying neuronal responses. Hence,

with additive IID noise and a maximum-likelihood decision rule, a change in the neuronal contrast-response functions would be accompanied by a similar change in performance accuracy. If the underlying neuronal responses showed an increase in response gain (Fig. 1B and C), the psychometric function would be scaled (Fig. 3A and B). If the underlying neuronal responses showed an increase in contrast gain, the psychometric function would shift horizontally (on the log contrast axis). Considering an alternative model of noise, in which performance is limited by the Poisson-like noise evident in single-cell firing rates (Carandini, 2004; Dean, 1981) together with a maximum-likelihood decision rule (Jazayeri & Movshon, 2006) yields the same interpretation of the psychometric functions (Pestilli, Ling, & Carrasco, 2009).

Using the normalization model of attention as a framework, the fact that there is a shift from response gain to contrast gain for spatial attention with smaller stimuli and broader attention fields (Herrmann et al., 2010), and not for FBA seems surprising at first, given that the spatial and feature domain are interchangeable in the model. However, to predict changes in contrast gain, it is crucial for the model simulations that the attention field be larger than both the excitatory stimulus drive and the suppressive drive. In the space domain, the attention field can be easily enlarged to such an extent. In the feature domain, however, the range of possible orientations is limited to 180°. The orientation-tuning bandwidths of neurons in visual cortex are ~40° (median full-width at half-max) (De Valois, Yund, & Hepler, 1982; Desimone & Schein, 1987; McAdams & Maunsell, 1999), and the suppressive fields (the range of orientations that contribute to suppression via normalization) are considerably broader (with all orientations contributing to the suppression), so the attention field cannot be much broader than the suppressive field. The model can simulate a change in contrast gain with FBA, but only for very narrow (biologically implausible) orientation bandwidths. For biologically plausible orientation-bandwidth values, the model predicts only a change in response gain for FBA to orientations. The model predicts that FBA to directions of motion should also yield changes in response gain, because neurons in area MT have even broader tuning bandwidths with a modal value of ~60–90° (Albright, 1984; Lagae, Raiguel, & Orban, 1993; Maunsell & Van Essen, 1983; Snowden, Treue, & Andersen, 1992), but this hypothesis will need to be experimentally tested in future studies.

#### 4.2. Neurophysiological correlates

We infer that performance in the present experiments, which involved directing FBA to spatially-distributed arrays of oriented gratings, may have relied on the responses of orientation-selective visual neurons in higher visual cortical areas in the ventral visual pathway, such as visual cortical area V4 (Desimone & Schein, 1987). Best-fitting values for the exponents of the psychometric functions were ~4, for both the low-uncertainty and high-uncertainty experiments. This range of exponents is similar to the range of values reported for contrast-response functions of neurons in V4 (Cheng et al., 1994; Sclar, Maunsell, & Lennie, 1990). Lower exponents (~2) were derived from previous psychophysical experiments on spatial attention with a parallel cueing and uncertainty protocol (Herrmann et al., 2010); those exponents were in the range of values report for contrast-response functions of neurons in V1 (Sclar, Maunsell, & Lennie, 1990).

A recent neurophysiological study has reported that FBA results in larger modulations at medium and high contrasts than at low contrasts (Khayat, Niebergall, & Martinez-Trujillo, 2010), in agreement with the present results. Unlike the tasks we used, however, the task used in the neurophysiology study did not fully exclude a spatial attention contribution. Responses in area MT were recorded while a pair of random-dot stimuli moved in the receptive field of

an MT neuron in one hemifield and another pair outside the receptive field, in the other hemifield. Each pair consisted of a high-contrast random-dot pattern moving in the neuron's anti-preferred direction and a second random-dot test pattern moving in the neuron's preferred direction, with different contrasts on different trials. The responses of MT neurons were measured when monkeys attended to fixation to detect luminance changes, and when attention was spatially directed to the stimulus pair outside the receptive field to detect a direction change in one of the two random dot patterns. Hence, the monkeys were cued to shift both spatial and FBA; differences in the distribution of spatial attention may have elevated sensory responses in the attend-fixation condition, thus exaggerating the degree of relative suppression when the more distant moving stimulus pair was attended.

#### 4.3. Featural attention field size

We found that the featural extent of the attention field can be manipulated by introducing uncertainty about the upcoming feature dimension. Thus, the featural extent of the attention field is flexible and observers are able to adjust it to the needs of the current task. Manipulating featural uncertainty affected performance accuracy and task difficulty. We ensured, however, that task difficulty did not confound the interpretation of our results by adjusting the degree of stimulus tilt separately for each observer and for the high and low uncertainty conditions, so that performance was approximately 75% correct at full contrast with a neutral cue. Moreover, we compared only the differences in performance accuracy for valid and invalid cues within each condition (low uncertainty, high uncertainty).

The spatial extent of the attention field has been reported to be flexible in size and has been experimentally manipulated by introducing uncertainty about the location of the upcoming target (Castiello & Umiltà, 1990; Datta & DeYoe, 2009; Eriksen & St James, 1986; Herrmann et al., 2010; Muller et al., 2003; Yigit-Elliott, Palmer, & Moore, 2011). This flexibility, however, had previously not been demonstrated for featural attention. Previous experiments have used uncertainty to show feature selectivity with regard to spatial frequency (Cormack & Blake, 1980; Davis & Graham, 1981; Davis, Kramer, & Graham, 1983; Graham, Robson, & Nachmias, 1978), but have not adjusted its size.

The control experiments verified that the uncertainty manipulation was effective. All observers performed consistently worse at near  $\pm 45^\circ$  orientations in the valid condition when there was high- than when there was low-uncertainty about the upcoming orientation (Fig. 5), indicating that observers used the pre-cue. With high uncertainty, observers spread attention across the larger pre-cued orientation range; they performed equally well at several orientation ranges across the full pre-cued range, and the attentional gain was evident at all pre-cued orientations, indicating a large featural extent of attention (Fig. 6A). With low uncertainty, performance was better for orientations that differed slightly from the pre-cued orientation than at the pre-cued orientation (Fig. 6B), indicating that the featural extent of attention was narrow. This finding is consistent with previous reports that for fine discriminations, performance is best when monitoring the responses of neurons that are tuned for a feature that differs slightly from the stimulus (Jazayeri & Movshon, 2006, 2007; Navalpakkam & Itti, 2007; Scolari & Serences, 2009). In our low-uncertainty experiment, we infer that attentional gain was largest for neurons tuned to  $\pm 45^\circ$ , because neurons that prefer  $\pm 45^\circ$  have tuning curves that are steepest at nearby orientations, thereby maximizing performance for those nearby orientations.

Future studies might explore whether and how the featural extent of the attention field influences the tuning width of visual neurons. FBA has been reported to not only scale neuronal re-

sponses (Treue & Martinez Trujillo, 1999), but also sharpen the tuning (Martinez-Trujillo & Treue, 2004). This finding has been supported by psychophysical studies for orientation (Baldassi & Verghese, 2005) and for directions of motion (Ling, Liu, & Carrasco, 2009). The normalization model of attention can also exhibit sharpened tuning. In the model, the degree of sharpening depends on the featural extent of the attention field; a small featural attention field sharpens the tuning more than a broad featural attention field (Reynolds & Heeger, 2009).

## 5. Conclusion

In this study we show that FBA modulates activity in visual cortex to stimulus contrast in a manner that resembles a change in response gain, both with a small and large featural extent of the attention field. This study also provides the first experimental evidence that the featural attention field can be manipulated. The present findings support key predictions of the normalization model of attention (Reynolds & Heeger, 2009), thereby furthering our understanding of the processing in visual cortex and the neural computations underlying visual attention.

## Acknowledgments

Supported by National Institutes of Health Grant R01-EY019693 to DJH and MC and R01-EY016200 to MC. We thank Norma Graham, Mike Landy, Brian McElree and Shani Offen and members of the Carrasco Lab and Heeger Lab for their comments on the manuscript and helpful discussions.

## References

- Adam, J. J., Ketelaars, M., Kingma, H., & Hoek, T. (1993). On the time course and accuracy of spatial localization: Basic data and a two-process model. *Acta Psychologica (Amst)*, 84(2), 135–159.
- Alais, D., & Blake, R. (1999). Neural strength of visual attention gauged by motion adaptation. *Nature Neuroscience*, 2(11), 1015–1018.
- Albright, T. D. (1984). Direction and orientation selectivity of neurons in visual area MT of the macaque. *Journal of Neurophysiology*, 52(6), 1106–1130.
- Averbeck, B. B., Latham, P. E., & Pouget, A. (2006). Neural correlations, population coding and computation. *Nature Reviews Neuroscience*, 7(5), 358–366.
- Baldassi, S., & Verghese, P. (2005). Attention to locations and features: Different top-down modulation of detector weights. *Journal of Vision*, 5(6), 556–570.
- Barlow, H. B., Kaushal, T. P., Hawken, M., & Parker, A. J. (1987). Human contrast discrimination and the threshold of cortical neurons. *Journal of the Optical Society of America A: Optics, Image Science, and Vision*, 4(12), 2366–2371.
- Ben-Av, M. B., & Sagi, D. (1995). Perceptual grouping by similarity and proximity: Experimental results can be predicted by intensity autocorrelations. *Vision Research*, 35(6), 853–866.
- Boynton, G. M. (2005). Attention and visual perception. *Current Opinion in Neurobiology*, 15(4), 465–469.
- Boynton, G. M. (2009). A framework for describing the effects of attention on visual responses. *Vision Research*, 49(10), 1129–1143.
- Boynton, G. M., Demb, J. B., Glover, G. H., & Heeger, D. J. (1999). Neuronal basis of contrast discrimination. *Vision Research*, 39(2), 257–269.
- Breitmeyer, B. G., & Ogmen, H. (2000). Recent models and findings in visual backward masking: A comparison, review, and update. *Perception & Psychophysics*, 62(8), 1572–1595.
- Buracas, G. T., & Boynton, G. M. (2007). The effect of spatial attention on contrast response functions in human visual cortex. *Journal of Neuroscience*, 27(1), 93–97.
- Carandini, M. (2004). Amplification of trial-to-trial response variability by neurons in visual cortex. *PLoS Biology*, 2(9), E264.
- Carandini, M., & Heeger, D. J. (2011). Normalization as a canonical neural computation. *Nature Reviews Neuroscience*.
- Carandini, M., Heeger, D. J., & Movshon, J. A. (1997). Linearity and normalization in simple cells of the macaque primary visual cortex. *Journal of Neuroscience*, 17(21), 8621–8644.
- Carrasco, M. (2011). Visual attention: The past 25 years. *Vision Research*.
- Carrasco, M., & Chang, I. (1995). The interaction of objective and subjective organizations in a localization search task. *Perception & Psychophysics*, 57(8), 1134–1150.
- Carrasco, M., Penpeci-Talgar, C., & Eckstein, M. (2000). Spatial covert attention increases contrast sensitivity across the CSF: Support for signal enhancement. *Vision Research*, 40(10–12), 1203–1215.
- Castiello, U., & Umiltà, C. (1990). Size of the attentional focus and efficiency of processing. *Acta Psychologica (Amst)*, 73(3), 195–209.
- Cavanaugh, J. R., Bair, W., & Movshon, J. A. (2002a). Nature and interaction of signals from the receptive field center and surround in macaque V1 neurons. *Journal of Neurophysiology*, 88(5), 2530–2546.
- Cavanaugh, J. R., Bair, W., & Movshon, J. A. (2002b). Selectivity and spatial distribution of signals from the receptive field surround in macaque V1 neurons. *Journal of Neurophysiology*, 88(5), 2547–2556.
- Cheng, K., Hasegawa, T., Saleem, K. S., & Tanaka, K. (1994). Comparison of neuronal selectivity for stimulus speed, length, and contrast in the prestriate visual cortical areas V4 and MT of the macaque monkey. *Journal of Neurophysiology*, 71(6), 2269–2280.
- Cormack, R. H., & Blake, R. (1980). Do the two eyes constitute separate visual channels? *Science*, 207(4435), 1100–1102.
- Datta, R., & DeYoe, E. A. (2009). I know where you are secretly attending! The topography of human visual attention revealed with fMRI. *Vision Research*, 49(10), 1037–1044.
- Davis, E. T., & Graham, N. (1981). Spatial frequency uncertainty effects in the detection of sinusoidal gratings. *Vision Research*, 21(5), 705–712.
- Davis, E. T., Kramer, P., & Graham, N. (1983). Uncertainty about spatial frequency, spatial position, or contrast of visual patterns. *Perception & Psychophysics*, 33(1), 20–28.
- De Valois, R. L., Yund, E. W., & Hepler, N. (1982). The orientation and direction selectivity of cells in macaque visual cortex. *Vision Research*, 22(5), 531–544.
- Dean, A. F. (1981). The variability of discharge of simple cells in the cat striate cortex. *Experimental Brain Research*, 44(4), 437–440.
- Desimone, R., & Schein, S. J. (1987). Visual properties of neurons in area V4 of the macaque: Sensitivity to stimulus form. *Journal of Neurophysiology*, 57(3), 835–868.
- Dumoulin, S. O., & Wandell, B. A. (2008). Population receptive field estimates in human visual cortex. *Neuroimage*, 39(2), 647–660.
- Eriksen, C. W., & St James, J. D. (1986). Visual attention within and around the field of focal attention: A zoom lens model. *Perception & Psychophysics*, 40(4), 225–240.
- Geisler, W. S., & Albrecht, D. G. (1997). Visual cortex neurons in monkeys and cats: Detection, discrimination, and identification. *Visual Neuroscience*, 14(5), 897–919.
- Gheri, C., & Baldassi, S. (2008). Non-linear integration of crowded orientation signals. *Vision Research*, 48(22), 2352–2358.
- Ghose, G. M. (2009). Attentional modulation of visual responses by flexible input gain. *Journal of Neurophysiology*, 101(4), 2089–2106.
- Gold, J. I., & Shadlen, M. N. (2001). Neural computations that underlie decisions about sensory stimuli. *Trends in Cognitive Sciences*, 5(1), 10–16.
- Gold, J. I., & Shadlen, M. N. (2007). The neural basis of decision making. *Annual Review of Neuroscience*, 30, 535–574.
- Gorea, A. (1987). Masking efficiency as a function of stimulus onset asynchrony for spatial-frequency detection and identification. *Spatial Vision*, 2(1), 51–60.
- Graham, N., Robson, J. G., & Nachmias, J. (1978). Grating summation in fovea and periphery. *Vision Research*, 18(7), 815–825.
- Haenny, P. E., Maunsell, J. H., & Schiller, P. H. (1988). State dependent activity in monkey visual cortex. II. Retinal and extraretinal factors in V4. *Experimental Brain Research*, 69(2), 245–259.
- Heeger, D. J. (1992). Normalization of cell responses in cat striate cortex. *Visual Neuroscience*, 9(2), 181–197.
- Herrmann, K., Montaser-Kouhsari, L., Carrasco, M., & Heeger, D. J. (2010). When size matters: Attention affects performance by contrast or response gain. *Nature Neuroscience*, 13(12), 1554–1559.
- Jazayeri, M., & Movshon, J. A. (2006). Optimal representation of sensory information by neural populations. *Nature Neuroscience*, 9(5), 690–696.
- Jazayeri, M., & Movshon, J. A. (2007). Integration of sensory evidence in motion discrimination. *Journal of Vision*, 7(12), 7.1–7.
- Joffe, K. M., & Scialfa, C. T. (1995). Texture segmentation as a function of eccentricity, spatial frequency and target size. *Spatial Vision*, 9(3), 325–342.
- Katkov, M., Tsodyks, M., & Sagi, D. (2007). Inverse modeling of human contrast response. *Vision Research*, 47(22), 2855–2867.
- Khayat, P. S., Niebergall, R., & Martinez-Trujillo, J. C. (2010). Attention differentially modulates similar neuronal responses evoked by varying contrast and direction stimuli in area MT. *Journal of Neuroscience*, 30(6), 2188–2197.
- Lagae, L., Raiguel, S., & Orban, G. A. (1993). Speed and direction selectivity of macaque middle temporal neurons. *Journal of Neurophysiology*, 69(1), 19–39.
- Lankheet, M. J., & Verstraten, F. A. (1995). Attentional modulation of adaptation to two-component transparent motion. *Vision Research*, 35(10), 1401–1412.
- Lee, J., & Maunsell, J. H. (2009). A normalization model of attentional modulation of single unit responses. *PLoS ONE*, 4(2), e4651.
- Li, X., Lu, Z. L., Tjan, B. S., Doshier, B. A., & Chu, W. (2008). Blood oxygenation level-dependent contrast response functions identify mechanisms of covert attention in early visual areas. *Proceedings of the National Academy of Sciences of the United States of America*, 105(16), 6202–6207.
- Ling, S., & Carrasco, M. (2006). Sustained and transient covert attention enhance the signal via different contrast response functions. *Vision Research*, 46(8–9), 1210–1220.
- Ling, S., Liu, T., & Carrasco, M. (2009). How spatial and feature-based attention affect the gain and tuning of population responses. *Vision Research*, 49(10), 1194–1204.
- Liu, T., Larsson, J., & Carrasco, M. (2007). Feature-based attention modulates orientation-selective responses in human visual cortex. *Neuron*, 55(2), 313–323.

- Liu, T., Pestilli, F., & Carrasco, M. (2005). Transient attention enhances perceptual performance and fMRI response in human visual cortex. *Neuron*, 45, 469–477.
- Liu, T., Stevens, S. T., & Carrasco, M. (2007). Comparing the time course and efficacy of spatial and feature-based attention. *Vision Research*, 47(1), 108–113.
- Lu, Z. L., & Doshier, B. A. (1998). External noise distinguishes attention mechanisms. *Vision Research*, 38(9), 1183–1198.
- Lu, Z. L., Li, X., Tjan, B. S., Doshier, B. A., & Chu, W. (2011). Attention extracts signal in external noise: A BOLD fMRI study. *Journal of Cognitive Neuroscience*, 23(5), 1148–1159.
- Martinez-Trujillo, J., & Treue, S. (2002). Attentional modulation strength in cortical area MT depends on stimulus contrast. *Neuron*, 35(2), 365–370.
- Martinez-Trujillo, J. C., & Treue, S. (2004). Feature-based attention increases the selectivity of population responses in primate visual cortex. *Current Biology*, 14(9), 744–751.
- Maunsell, J. H., & Treue, S. (2006). Feature-based attention in visual cortex. *Trends in Neurosciences*, 29(6), 317–322.
- Maunsell, J. H., & Van Essen, D. C. (1983). Functional properties of neurons in middle temporal visual area of the macaque monkey. I. Selectivity for stimulus direction, speed, and orientation. *Journal of Neurophysiology*, 49(5), 1127–1147.
- McAdams, C. J., & Maunsell, J. H. (1999). Effects of attention on orientation-tuning functions of single neurons in macaque cortical area V4. *Journal of Neuroscience*, 19(1), 431–441.
- McAdams, C. J., & Reid, R. C. (2005). Attention modulates the responses of simple cells in monkey primary visual cortex. *Journal of Neuroscience*, 25(47), 11023–11033.
- Morrone, M. C., Denti, V., & Spinelli, D. (2002). Color and luminance contrasts attract independent attention. *Current Biology*, 12(13), 1134–1137.
- Morrone, M. C., Denti, V., & Spinelli, D. (2004). Different attentional resources modulate the gain mechanisms for color and luminance contrast. *Vision Research*, 44(12), 1389–1401.
- Motter, B. C. (1994a). Neural correlates of attentive selection for color or luminance in extrastriate area V4. *Journal of Neuroscience*, 14(4), 2178–2189.
- Motter, B. C. (1994b). Neural correlates of feature selective memory and pop-out in extrastriate area V4. *Journal of Neuroscience*, 14(4), 2190–2199.
- Muller, N. G., Bartelt, O. A., Donner, T. H., Villringer, A., & Brandt, S. A. (2003). A physiological correlate of the “Zoom Lens” of visual attention. *Journal of Neuroscience*, 23(9), 3561–3565.
- Murray, S. O., & He, S. (2006). Contrast invariance in the human lateral occipital complex depends on attention. *Current Biology*, 16(6), 606–611.
- Navalpakkam, V., & Itti, L. (2007). Search goal tunes visual features optimally. *Neuron*, 53(4), 605–617.
- Parkes, L., Lund, J., Angelucci, A., Solomon, J. A., & Morgan, M. (2001). Compulsory averaging of crowded orientation signals in human vision. *Nature Neuroscience*, 4(7), 739–744.
- Pestilli, F., & Carrasco, M. (2005). Attention enhances contrast sensitivity at cued and impairs it at uncued locations. *Vision Research*, 45(14), 1867–1875.
- Pestilli, F., Carrasco, M., Heeger, D. J., & Gardner, J. L. (2011). Attentional enhancement via selection and pooling of early sensory responses in visual cortex. *Neuron*, 72, 832–846.
- Pestilli, F., Ling, S., & Carrasco, M. (2009). A population-coding model of attention's influence on contrast response: Estimating neural effects from psychophysical data. *Vision Research*, 49(10), 1144–1153.
- Pestilli, F., Viera, G., & Carrasco, M. (2007). How do attention and adaptation affect contrast sensitivity? *Journal of Vision*, 7(7), 9.1–12.
- Reynolds, J. H., & Chelazzi, L. (2004). Attentional modulation of visual processing. *Annual Review of Neuroscience*, 27, 611–647.
- Reynolds, J. H., & Heeger, D. J. (2009). The normalization model of attention. *Neuron*, 61(2), 168–185.
- Reynolds, J. H., Pasternak, T., & Desimone, R. (2000). Attention increases sensitivity of V4 neurons. *Neuron*, 26(3), 703–714.
- Rogowitz, B. E. (1983). Spatial/temporal interactions: Backward and forward metacontrast masking with sine-wave gratings. *Vision Research*, 23(10), 1057–1073.
- Ross, J., & Speed, H. D. (1991). Contrast adaptation and contrast masking in human vision. *Proceedings of the Royal Society of London B: Biological Sciences*, 246, 61–69.
- Saenz, M., Buracas, G. T., & Boynton, G. M. (2002). Global effects of feature-based attention in human visual cortex. *Nature Neuroscience*, 5(7), 631–632.
- Saenz, M., Buracas, G. T., & Boynton, G. M. (2003). Global feature-based attention for motion and color. *Vision Research*, 43(6), 629–637.
- Scial, G., Maunsell, J. H., & Lennie, P. (1990). Coding of image contrast in central visual pathways of the macaque monkey. *Vision Research*, 30(1), 1–10.
- Scolari, M., & Serences, J. T. (2009). Adaptive allocation of attentional gain. *Journal of Neuroscience*, 29(38), 11933–11942.
- Serences, J. T., & Boynton, G. M. (2007). Feature-based attentional modulations in the absence of direct visual stimulation. *Neuron*, 55(2), 301–312.
- Serences, J. T., Saproo, S., Scolari, M., Ho, T., & Muftuler, L. T. (2009). Estimating the influence of attention on population codes in human visual cortex using voxel-based tuning functions. *Neuroimage*, 44(1), 223–231.
- Shadlen, M. N., Britten, K. H., Newsome, W. T., & Movshon, J. A. (1996). A computational analysis of the relationship between neuronal and behavioral responses to visual motion. *Journal of Neuroscience*, 16(4), 1486–1510.
- Shadlen, M. N., & Newsome, W. T. (1998). The variable discharge of cortical neurons: Implications for connectivity, computation, and information coding. *Journal of Neuroscience*, 18(10), 3870–3896.
- Snowden, R. J., Treue, S., & Andersen, R. A. (1992). The response of neurons in areas V1 and MT of the alert rhesus monkey to moving random dot patterns. *Experimental Brain Research*, 88(2), 389–400.
- Spering, M., & Carrasco, M. (in press). Similar effects of feature-based attention on motion perception and pursuit eye movements at different levels of awareness. *Journal of Neuroscience*.
- Spitzer, H., Desimone, R., & Moran, J. (1988). Increased attention enhances both behavioral and neuronal performance. *Science*, 240(4850), 338–340.
- Spivey, M. J., & Spirn, M. J. (2000). Selective visual attention modulates the direct tilt aftereffect. *Perception & Psychophysics*, 62(8), 1525–1533.
- Treue, S., & Martinez Trujillo, J. C. (1999). Feature-based attention influences motion processing gain in macaque visual cortex. *Nature*, 399(6736), 575–579.
- Treue, S., & Maunsell, J. H. (1999). Effects of attention on the processing of motion in macaque middle temporal and medial superior temporal visual cortical areas. *Journal of Neuroscience*, 19(17), 7591–7602.
- Watson, A. B., & Pelli, D. G. (1983). QUEST: A Bayesian adaptive psychometric method. *Perception & Psychophysics*, 33(2), 113–120.
- White, A. L., & Carrasco, M. (2011). Feature-based attention involuntarily and simultaneously improves visual performance across locations. *Journal of Vision*, 11(6).
- Williford, T., & Maunsell, J. H. (2006). Effects of spatial attention on contrast response functions in macaque area V4. *Journal of Neurophysiology*, 96(1), 40–54.
- Yigit-Elliott, S., Palmer, J., & Moore, C. M. (2011). Distinguishing blocking from attenuation in visual selective attention. *Psychological Science*, 22(6), 771–780.